

# Telomere-independent homologue pairing and checkpoint escape of accessory ring chromosomes in male mouse meiosis

Thierry Voet,<sup>1</sup> Bodo Liebe,<sup>2</sup> Charlotte Labaere,<sup>1</sup> Peter Marynen,<sup>1</sup> and Harry Scherthan<sup>2</sup>

<sup>1</sup>Human Genome Laboratory, Department of Human Genetics, Flanders Interuniversity Institute for Biotechnology, University of Leuven, B-3000 Leuven, Belgium

<sup>2</sup>Max-Planck-Institute for Molecular Genetics, D-14195 Berlin, Germany

We analyzed transmission of a ring minichromosome (MC) through mouse spermatogenesis as a monosome and in the presence of a homologue. Mice, either monosomic or disomic for the MC, produced MC<sup>+</sup> offspring. In the monosomic condition, most univalents underwent self-synapsis as indicated by STAG3, SCP3, and SCP1 deposition. Fluorescent *in situ* hybridization and three-dimensional fluorescence microscopy revealed that ring MCs did not participate in meiotic telomere clustering while MC homologues paired at the XY-body periphery. Self-synapsis of MC(s) and association with the XY-body

likely allowed them to pass putative pachytene checkpoints. At metaphase I and II, MC kinetochores assembled MAD2 and BUBR1 spindle checkpoint proteins. Unaligned MCs triggered the spindle checkpoint leading to apoptosis of metaphase cells. Other MCs frequently associated with mouse pericentric heterochromatin, which may have allowed them to pass the spindle checkpoint. Our findings indicate a telomere-independent mechanism for pairing of mammalian MCs, illuminate escape routes to meiotic checkpoints, and give clues for genetic engineering of germ line-permissive chromosomal vectors.

## Introduction

Meiosis is a succession of two cell divisions by which the chromosome number is reduced from diploid to haploid to compensate for the genome doubling at fertilization. During the extended prophase of meiosis I, replicated homologous chromosomes (homologues) extend (leptotene), align, and initiate pairing (zygotene). Once pairing is complete (pachytene), there is only half the number of chromosomes than entered prophase I. During the first meiotic prophase, homologues undergo genetic exchange, which ensures their correct segregation during metaphase I (MI). During the second meiotic division, sister chromatids segregate to opposite poles, thereby forming haploid gametes or spores (von Wettstein et al., 1984; McKim and Hawley, 1995).

In most (if not all) organisms, meiotic telomeres cluster at the nuclear envelope during the leptotene/zygotene transition, which is known as the bouquet stage (Scherthan, 2001; Yamamoto and Hiraoka, 2001). Clustering of chromosome ends is thought to instigate homologue interactions and regional presynaptic alignment, which is transformed into stable pairing by the synaptonemal complex (SC; Zickler and Kleckner, 1998). The SC consists of two lateral elements (LE) that run along the sister chromatids of replicated homologues, and a central element that is formed by transverse filaments connecting the LEs (von Wettstein et al., 1984). Before synapsis, the LEs are called axial elements (AE). Three SC proteins have been characterized in mammals: SCP2 (Offenberg et al., 1998) and SCP3 (Lammers et al., 1994; Yuan et al., 1998), which both are components of the AE/LE (Schalk et al., 1998; Yuan et al., 2000), and SCP1 (Meuwissen et al., 1992), which is a major component of transverse filaments (Schmekel et al., 1996).

T. Voet and B. Liebe contributed equally to this paper.

Address correspondence to Harry Scherthan, Max-Planck-Institute for Molecular Genetics, Dept. Ropers, D-14195 Berlin, Germany. Tel.: 49-30-8413-1251. Fax: 49-89-8413-8313.

email: schertha@molgen.mpg.de; or Peter Marynen, Center for Human Genetics, Flanders Interuniversity Institute for Biotechnology, University of Leuven, B-3000 Leuven, Belgium. email: peter.marynen@Med.Kuleuven.ac.be

Key words: chromosomal vector; spindle checkpoint; bouquet; synapsis; sex body

Abbreviations used in this paper: 3D, three dimensional; AE, axial element; DSB, DNA double-strand break; IF, immunofluorescent; LE, lateral element; MC, minichromosome; MI, metaphase I; MII, metaphase II; PNA, peptide nucleic acid; SC, synaptonemal complex.

AEs are built on cohesin cores that form after premeiotic DNA replication and consist of different subunits (SMC1 $\alpha$ , SMC1 $\beta$ , SMC3, REC8, and STAG3; Prieto et al., 2001, 2002; Revenkova et al., 2001; Eijpe et al., 2003). The separation of homologues is achieved by removal of sister chromatid cohesion along chromosome arms at the onset of anaphase I, whereas cohesion at sister centromeres is lost at anaphase II (Buonomo et al., 2000; Petronczki et al., 2003). The complex events in meiotic differentiation are under checkpoint control, and meiotic disturbances elicit different responses in male and female mammals (Hunt and Hassold, 2002), which often prevent efficient germ line transmission of accessory (mini)chromosomes in murine spermatogenesis (Voet et al., 2001). Furthermore, knockout mice for genes involved in recombination and synapsis display sex-specific responses, with male gametogenesis often grinding to a halt during prophase I (Escalier, 2001; Hunt and Hassold, 2002). These observations have provided evidence for mammalian "pachytene" checkpoints that respond to defective meiotic recombination and/or synapsis in spermatocytes in a p53-dependent or -independent manner (Odorisio et al., 1998; Cohen and Pollard, 2001).

Furthermore, there is evidence for a spindle assembly checkpoint that operates at MI in mice, which responds to kinetochores that fail to attach or are not under tension (Woods et al., 1999; Sluder and McCollum, 2000). Thus, introduction of artificial chromosomes into a mammalian genome can be used to test crucial aspects of meiotic chromosome behavior and checkpoints.

Recently, we have generated "transchromosomal" mice carrying a chromosomal vector in the form of a small accessory human minichromosome (human MC, previously termed HCV; Voet et al., 2001). This MC consists mainly of alphoid sequences of the human chromosome 20, a fragment of the human chromosome 1p22 region, and lacks telomere sequences (Voet et al., 2001). Most surprisingly, both male and female mice carrying the MC (MC<sup>+</sup> mice) efficiently transmit the univalent MC to the offspring (Voet et al., 2001), even when a large transgene insert is present in the MC (Voet et al., 2003). Here, we analyze which checkpoint responses are elicited by the presence of a monosomic or disomic circular MC in spermatogenesis, test the role of telomeres for the pairing of ring minichromosomes, and disclose mechanisms that enable MCs to bypass meiotic checkpoints.

Table I. Frequency of MC<sup>+</sup> primary tail fibroblast metaphases

Mice		Percentage of MC <sup>+</sup> tail fibroblasts				
		0 MCs	1 MC	2 MCs	3 MCs	4 MCs
		%	%	%	%	%
Monosomic	1MC <sup>+</sup> -28	13	87	-	-	-
	1MC <sup>+</sup> -39	17	77	4	2	-
	1MC <sup>+</sup> -9	45	54	1	-	-
	1MC <sup>+</sup> -20	12	86	2	-	-
	1MC <sup>+</sup> -11	22	78	-	-	-
	1MC <sup>+</sup> -23	26	68	6	-	-
	1MC <sup>+</sup> -7	34	62	4	-	-
	1MC <sup>+</sup> -6	28	69	3	-	-
	1MC <sup>+</sup> -30	22	78	-	-	-
Disomic	2MC <sup>+</sup> -7	6	38	52	3	1
	2MC <sup>+</sup> -10	6	28	59	6	1
	2MC <sup>+</sup> -35	5	46	48	1	-
	2MC <sup>+</sup> -4	4	19	29	46	2
	2MC <sup>+</sup> -6	5	24	41	30	-
	2MC <sup>+</sup> -13	12	46	39	3	-
	2MC <sup>+</sup> -16	16	48	32	2	2

## Results

### MC<sup>+</sup> mice and offspring

MC<sup>+</sup> mice, generated previously (Voet et al., 2001), were used to breed the MC into the C57Bl/6 and NMRI genetic background. Up to now, a total of 17 male mice, containing one copy of the MC, have produced 1,115 offspring, 308 of which inherited the MC. Mice with a second copy of the MC were generated by mating MC<sup>+</sup> mice (Table I). For simplicity, mice (or cells) containing one copy of the MC are referred to as monosomic mice, and mice harboring two MC copies in most of their cells are designated as disomic mice.

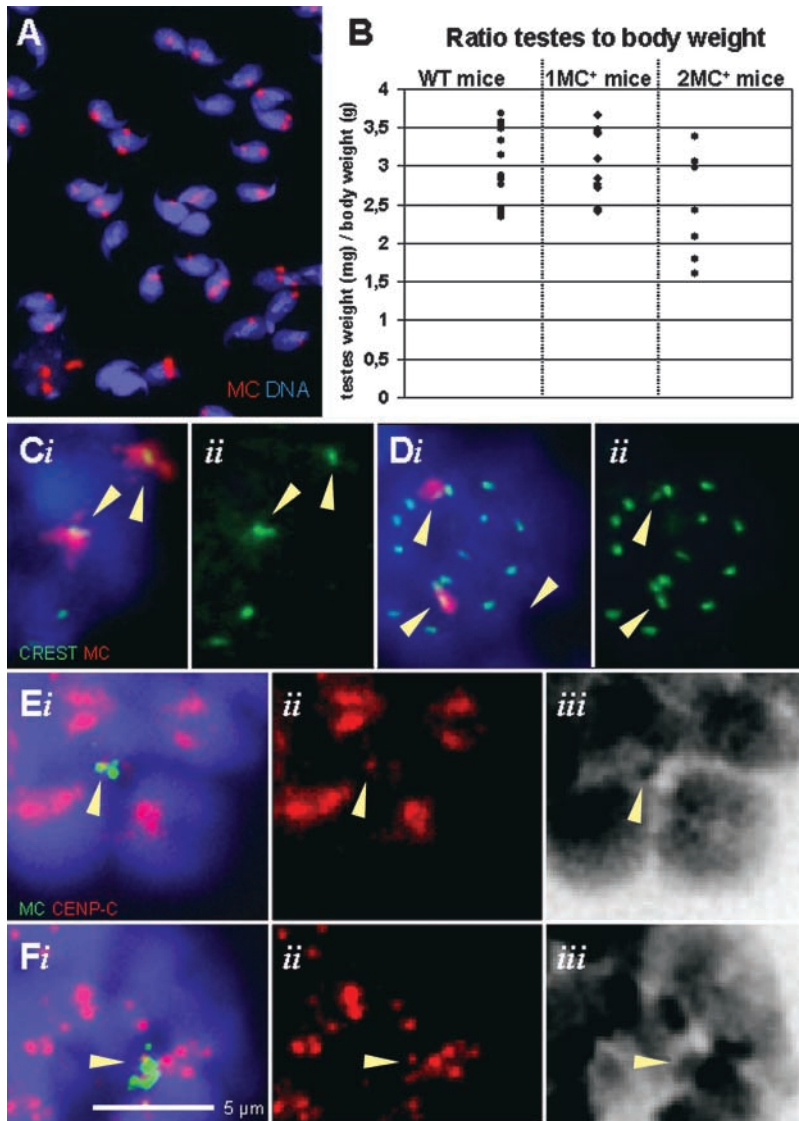
All monosomic and disomic MC<sup>+</sup> mice of both sexes tested so far produced live MC<sup>+</sup> offspring when mated to wild-type mice. Additionally, meiotic MC missegregation occurred in disomic mice of both sexes because part of their offspring harbored two MCs when mated to wild-type mice (Table II) and because 8–37% of their sperm nuclei ( $n \geq 100$ /animal) contained two or more MCs (Table III; Fig. 1 A). However, the MC-carrying males displayed similar testes weights (ANOVA combined with post-hoc test; P values > 0.16; Fig. 1 B).

Table II. Transmission of MCs in disomic male and female NMRI wild-type crosses

Parents	Disomic offspring	MC <sup>+</sup> primary tail fibroblast cells				
		0 MCs	1 MC	2 MCs	3 MCs	4 MCs
		%	%	%	%	%
Disomic male mated with NMRI female <sup>a</sup>	Mouse A	11	39	50	-	-
	Mouse B	7	37	57	-	-
	Mouse C	15	44	38	3	-
Disomic female mated with NMRI male <sup>b</sup>	Mouse D	15	41	44	-	-
	Mouse E	14	36	50	-	-
	Mouse F	13	49	38	-	-

<sup>a</sup>One litter of nine pups was analyzed. Four descendants had one MC, three (A–C) had predominantly two MCs.

<sup>b</sup>One litter of fourteen pups was analyzed. Four descendants had one MC, three (D–F) had predominantly two MCs.



**Figure 1. MC centromeres and segregation.** (A) MC-specific  $\alpha$ -satellite DNA FISH (red) on sperm of a disomic mouse. Spermheads with 1–3 MC signals are detected. (B) Testes to body weight ratios (mg/g) of wild-type ( $n = 13$ ), monosomic ( $n = 11$ ), and disomic ( $n = 7$ ) mice. (C and D) IF staining for CREST (green) combined with  $\alpha$ -satellite MC FISH (red) on metaphase I (C) and II (D) nuclei. (E and F) CENP-C IF staining signals detected at the FISH-labeled CV in prometaphase I (E) and II (F) nuclei. Arrowheads in C–F denote MC FISH signals and their respective kinetochore signals. (Eiii and Fiii) Inverted grayscale DAPI channel.

### Meiotic MCs contain active centromeres, but no telomeres

Because the data above show that MCs are able to bypass the stringent male meiotic control checkpoints, a feature that is

rarely encountered in mammalian spermatogenesis (see Introduction), we next analyzed how the MC segregated through male meiosis in the monosomic or disomic condition.

First, we determined whether the MC is endowed with a functional centromere during meiosis and thus subject to checkpoint response. To this end, we performed combinatorial MC-specific FISH and immunofluorescent (IF) staining with either CREST antiserum or an anti-CENP-C antibody. Both types of experiments yielded dotlike signals on MCs in meiotic MI and metaphase II (MII; Fig. 1, C–F). Furthermore, we observed the presence of MAD2 and BUBR1 at MC kinetochores (see below).

FISH with a peptide nucleic acid (PNA) telomere probe to mitotic and meiotic metaphase chromosomes failed to detect telomere FISH signals at the MC (Voet et al., 2001). Similarly, IF staining with antibodies to TRF1 telomere repeat-binding factor (Broccoli et al., 1997) or mRap1 (Li et al., 2000) telomere proteins, which both stain meiotic telomeres (Scherthan et al., 2000), generated telomere signals at mouse SC ends, but failed to reveal telomere protein signals at the MCs (unpublished data). Furthermore, the MC resisted attempts to resolve it by pulsed-field gel electrophore-

Table III. FISH analysis of spermheads

Mice	MC <sup>+</sup> sperm nuclei	MC <sup>+</sup> sperm nuclei				
		0 MCs	1 MC	2 MCs	3 MCs	4 MCs
		%	%	%	%	%
Monosomic	1MC <sup>+</sup> -28	66	34	-	-	-
	1MC <sup>+</sup> -39	61	39	-	-	-
	1MC <sup>+</sup> -9	71	28	1	-	-
	1MC <sup>+</sup> -20	63	36	1	-	-
	1MC <sup>+</sup> -11	75	25	-	-	-
	1MC <sup>+</sup> -23	74	26	-	-	-
	1MC <sup>+</sup> -7	91	9	-	-	-
Disomic	1MC <sup>+</sup> -21	71	28	1	-	-
	2MC <sup>+</sup> -35	41.4	50.6	7.6	0.4	-
	2MC <sup>+</sup> -4	23	45.4	25.4	5.8	0.4
	2MC <sup>+</sup> -6	16	47	35	2	-

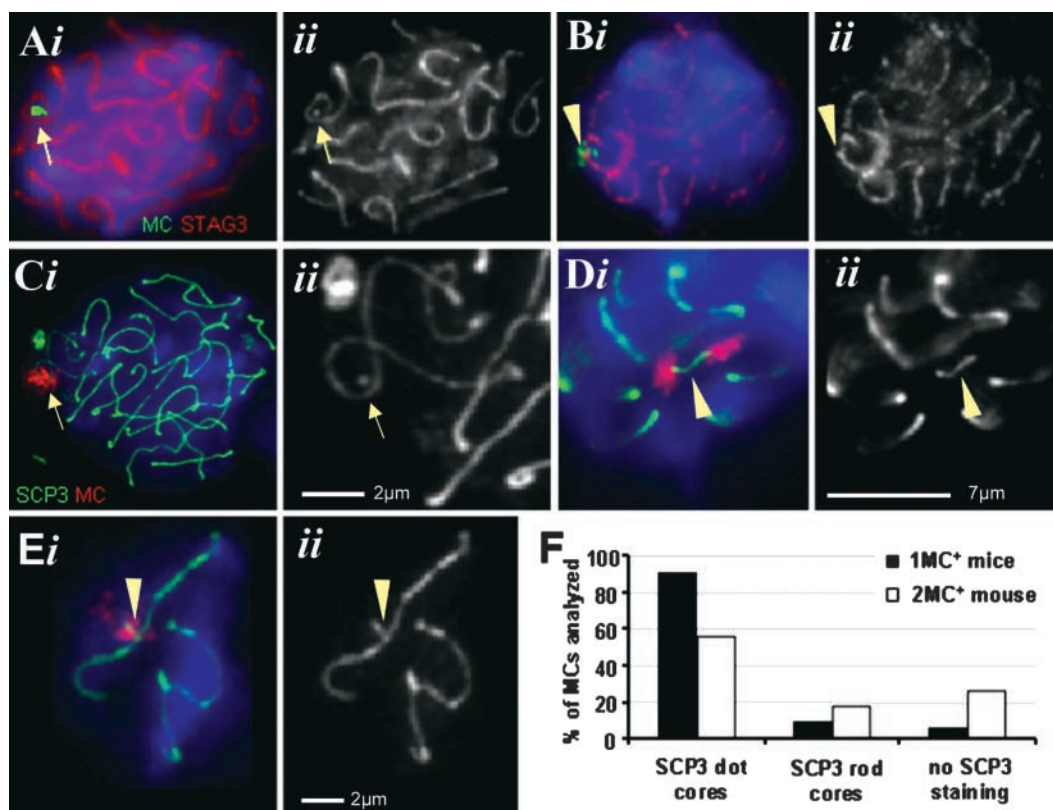


**Figure 2. MCs assemble a cohesin and AE core.** (A) IF staining for STAG3 (red) combined with MC FISH (green) on a monosomic pachytene nucleus. (Aii and Eii) Details showing the respective chromosome core in grayscale. A dotlike STAG3 signal (arrow) is present on the MC. (B) A connecting STAG3-positive structure (arrowhead) between the MC and the cohesin core of a monosomic mouse bivalent. (C–E) IF staining for SCP3 (green) combined with  $\alpha$ -satellite MC FISH (red) on pachytene nuclei. (C) A dotlike SCP3 signal (arrow) is detected at the MC in a monosomic spermatocyte nucleus close to the LE of the X chromosome. (Cii) Enlarged detail showing the chromosome core (arrow). (D) A SCP3 rod (arrowhead) connects two MCs in a spermatocyte I of a disomic mouse (note that this is the most extended rod observed). (E) A rodlike SCP3-positive structure (arrowhead) connects the MC with the SC of a monosomic mouse bivalent. (A–E) Images were taken of three-dimensionally preserved nuclei such that the focal planes were at the position of the SCP or STAG3 signals. Bars in Cii and Eii represent 2  $\mu$ m; bar in Dii is 7  $\mu$ m. (F) Frequencies of the SCP3 dot- and rodlike staining (based on  $\geq 50$  nuclei).

sis, which is expected for a ring chromosome of this size. These and the following observations indicate that the artificial chromosome is a ring chromosome that contains a functional centromere.

### MCs assemble SC protein structures

The fertility of MC<sup>+</sup> mice suggests germ line transmission in the presence of one and two (or multiple) MC copies. However, unpaired chromosome cores and absence of recombination appear to have the potential to trigger apoptosis through checkpoint activation in mammalian prophase I (for review see Cohen and Pollard, 2001). Two proteinaceous chromosome core structures, the AE/LE and the cohesin core (Peltari et al., 2001; Prieto et al., 2002), contribute to correct meiotic chromosome segregation (Petronczki et al., 2003). To investigate whether the MC assembles meiotic chromosome cores, we combined MC-specific FISH with IF staining of STAG3 (a component of meiotic cohesin cores), and SCP3 or SCP1 (SC components) on monosomic and disomic pachytene nuclei. Dotlike STAG3 cohesin signals were seen at 82% of the monosomic nuclei ( $n = 40$ ; Fig. 2 A), whereas in 15% of the nuclei, a STAG3 signal spanned between the univalent MC and the cohesin core of an adjacent bivalent (Fig. 2 B).

SCP3 IF staining produced signal dots at the MCs of monosomic and disomic spermatocytes (Fig. 2, C and F). 18% of disomic pachytene nuclei showed SCP3 rods between two closely associated MCs (Fig. 2, D and F) that measured 0.6  $\mu$ m (SD  $\pm$  0.06  $\mu$ m). Interestingly, in 14% of monosomic pachytene nuclei, SCP3 rods spanned between the univalent MC and the SC of a nearby bivalent (Fig. 2, E and F). The rodlike SCP3 structures suggest that the cohesin and SCP3 dot-cores of individual MCs may serve as a nucleation point for AE polymerization until contact is made to an AE/LE of a neighboring chromosome or to another dot-core on a homologous MC.

Immunostaining of SCP1, a marker for synapsis (Meuwissen et al., 1992; Dobson et al., 1994), revealed a dotlike SCP1 signal at the MC (Fig. 3, F and I) in 73% of the monosomic pachytene nuclei ( $n = 100$ ), which suggests that univalent MCs undergo self-synapsis and thereby evade checkpoint control.

In disomic MC<sup>+</sup> spermatocytes, combined SCP1 IF staining and MC-FISH disclosed that SCP1-positive structures connect two MCs in 78% of spermatocytes ( $n = 109$ ). The SCP1 mini-cores (Fig. 3, A–D and J) measured 0.64  $\mu$ m (SD  $\pm$  0.066  $\mu$ m) in 61% of cases ( $n = 66$ ; Fig. 3, B, C, and J), which agrees with the size of the SCP3 rods noted above. In

the remaining nuclei, a dotlike SCP1 signal ( $<0.5 \mu\text{m}$ ; Fig. 3, A, D, and J) was present between two MCs, whereas 11% of juxtaposed MCs failed to exhibit a SCP1 connection. Nuclei with two individual, closely spaced MC signals showed either one SCP1 dot at each MC (Fig. 3, E, G, and J) or no signal at all (Fig. 3 J). The high frequency of the SCP1 rods suggests that SCP1 can extend between SCP3 dot cores because SCP3 rods were only seen in 18% of nuclei.

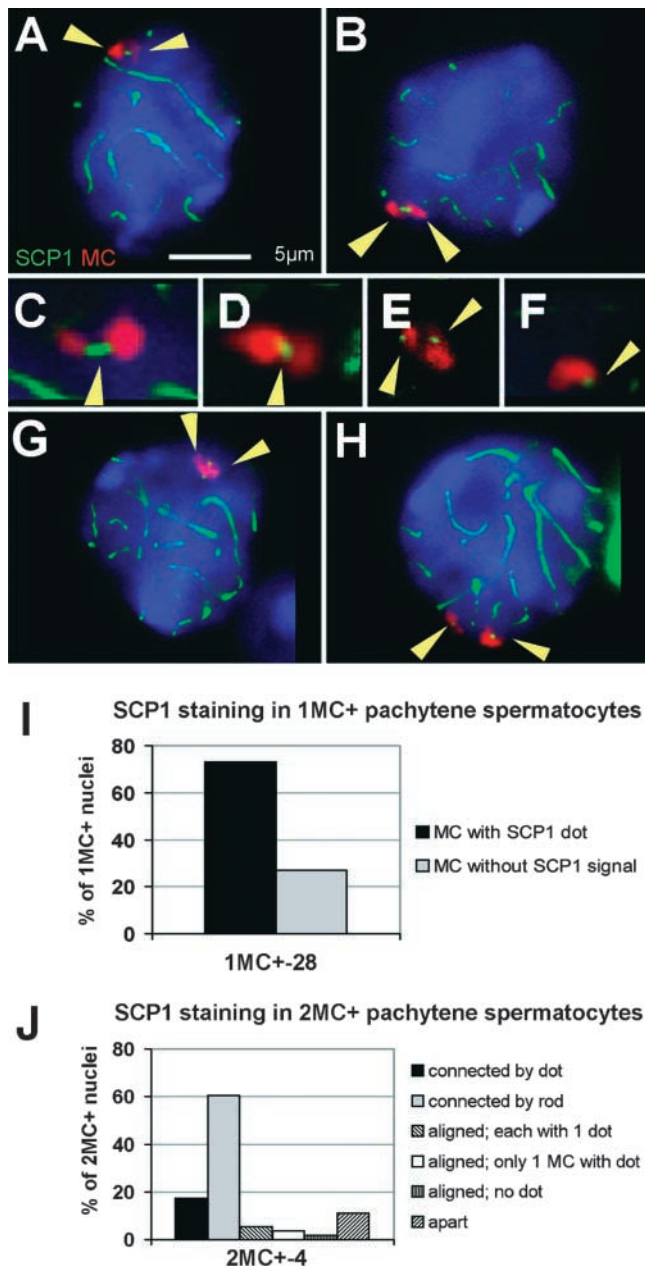


Figure 3. **MCPs contain SCP1.** (A–E, G, and H) Disomic pachytene spermatocytes stained for SCP1 (green; IF staining; arrowheads in C–F) and the MC (red; FISH; arrowheads in A, B, G, and H) show either dotlike SCP1 signals at separate (H), juxtaposed (E), and paired (G) MCPs, or rodlike (B and C) and dotlike (A and D) SCP1 cores between MCPs. The bar in A represents  $5 \mu\text{m}$  and also applies to B, G, and H. (F) Dotlike SCP1 signal (arrowhead) detected at the MC of a monosomic pachytene spermatocyte. (I and J) Frequencies of the different SCP1 staining patterns in monosomic and disomic pachytene nuclei.

Table IV. **Mono- or disomic MCPs do not trigger the pachytene checkpoint**

Mice		Mean number of apoptotic cells in stage I–XI tubules	Number of stage I–XI tubules analyzed
Wild-type	MC <sup>-</sup> -75	2.2	22
	MC <sup>-</sup> -79	1.4	23
Monosomic	1MC <sup>+</sup> -64	1	21
	1MC <sup>+</sup> -66	0.5	20
	1MC <sup>+</sup> -73	2.4	21
Disomic	2MC <sup>+</sup> -4	1.9	10
	2MC <sup>+</sup> -6	1.25	20

Because MCPs without SCP1 labeling have the potential to trigger the putative pachytene checkpoint, we investigated seminiferous tubules of stages I to XI of testes tissue sections (that harbor pachytene spermatocytes; Oakberg, 1956) for apoptotic cells by TUNEL assay. However, no significant differences were detected between the frequencies of apoptotic cells between monosomic, disomic, and wild-type stage I–XI tubules (Table IV). This suggests that monosomic and disomic MCPs efficiently transit through prophase I, with the disomic MCPs obviously undergoing an authentic mode of synaptonemal pairing.

#### Telomere-independent homologue pairing of MCPs

The pairing of the small MCPs (estimated size of 10–15 Mb) in the huge mouse spermatocyte nucleus poses the question of how the small MCPs associate with each other, especially because MCP-FISH revealed that they are spatially separated in premeiotic cells (in  $>80\%$  of disomic MCP<sup>+</sup> spermatogonia). At preleptotene, centromeres relocate to the nuclear periphery (Scherthan et al., 1996). In preleptotene nuclei of HMC<sup>+</sup> mice, MCPs were also found to follow these movements: three-dimensional (3D) microscopy revealed that 88% of the monosomic and 75% of the disomic preleptotene spermatocytes displayed peripheral MCP(s) (unpublished data). In disomic preleptotene spermatocytes, only 13% of peripheral MCPs were closely associated. Thus, MCPs, just like authentic centromeres, transit to the nuclear envelope during preleptotene, and they apparently pair later in prophase I.

A potential mechanism to instigate meiotic chromosome pairing is meiotic telomere clustering or bouquet formation (Scherthan, 2001; Yamamoto and Hiraoka, 2001). Thus, we prepared three-dimensionally preserved nuclei from testes of monosomic and disomic MCP<sup>+</sup> mice 12 d post partum, which are moderately enriched in bouquet stage nuclei. Two-color FISH with a (T<sub>2</sub>AG<sub>3</sub>)<sub>n</sub> telomere and an MCP-specific alphoid probe was used to identify bouquet nuclei with telomeres clustered in a limited region of the nuclear periphery, which also contain a few peripheral DAPI-bright heterochromatin masses (Scherthan et al., 1996). It was found that 97% of monosomic bouquet stage nuclei ( $n = 34$ ) displayed the MCP away from the bouquet base (Fig. 4, A and E). In the remaining nucleus, the MCP was detected at the telomere cluster (Fig. 4, B and E). In all but one disomic bouquet nuclei, both MCPs located away from the telomere-cluster site ( $n = 16$ ; Fig. 4, C–E). Although the MCPs failed

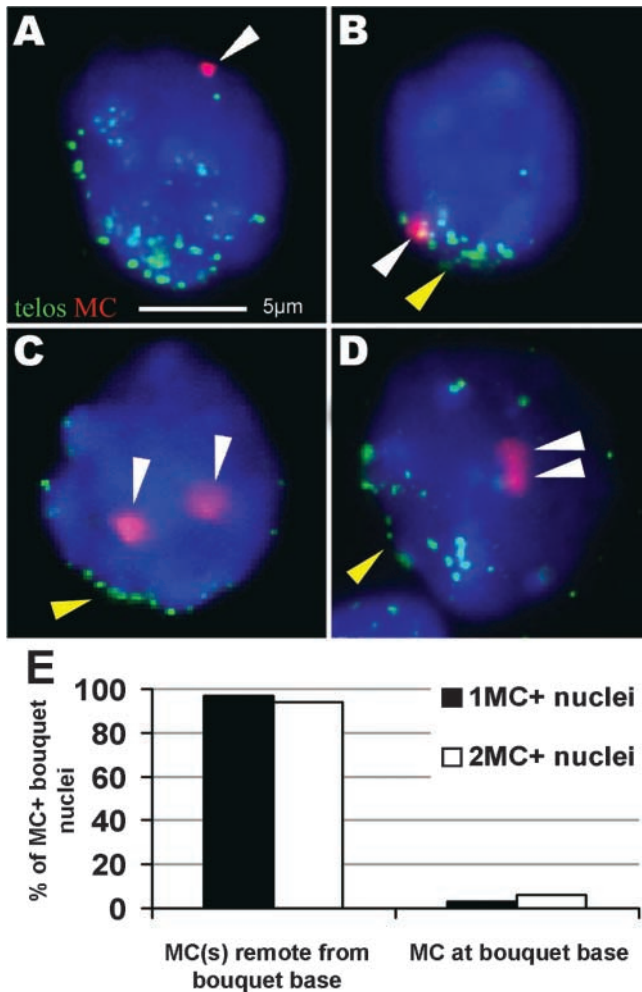


**Figure 4. MCs locate remote from the telomere cluster in bouquet nuclei.** (A and B) FISH with a  $(C_3TA_2)_3$  PNA telomere probe (green) and an  $\alpha$ -satellite DNA MC probe (red; white arrowhead) on monosomic bouquet stage nuclei ( $1MC^+$ -30; 12 d post partum). (A) A spermatocyte I with one MC located remote from the telomere cluster at the top of the nucleus (the latter faces the observer). (B) Spermatocyte with the MC located among the tightly clustered telomeres at the bouquet base (yellow arrowhead). Focal plane near the nuclear top. (C and D) Bouquet stage nuclei of a 12-d post partum disomic mouse ( $2MC^+$ -7). (C) Two separate MCs (white arrowheads) located away from the bouquet base (yellow arrowhead). Focal plane at nuclear equator. (D) Spermatocyte I nucleus with relaxed telomere clustering and two paired MCs (white arrowheads) that create a single large MC signal in the nuclear interior below. Focal plane at the nuclear top. The bar in A represents 5  $\mu$ m and applies to A–D. (E) Distribution frequencies of MCs with respect to the telomere cluster site. Two MCs were generally absent from the telomere cluster region.

to locate to the bouquet base, both MC signals coalesced in half of the nuclei analyzed. These data suggest that human ring minichromosomes that lack both functional telomeres and premeiotic homologue association still align and synapse with their homologue partner in mouse prophase I.

#### MCs associate with the XY body

The data above are suggestive for the presence of a bouquet-independent mode of chromosome alignment and pairing, at least for MCs. Similar numbers of apoptotic spermatocytes in

stage I–XI seminiferous tubules of monosomic, disomic, and wild-type mice (Table IV) indicate that MCs manage to bypass checkpoints that putatively monitor synapsis and/or DNA double-strand break (DSB) repair (Roeder and Bailis, 2000; Cohen and Pollard, 2001). A subcompartment of the spermatocyte I nucleus that tolerates the presence of asynapsed chromosome cores is the XY body (Jablonka and Lamb, 1988; Turner et al., 2000). Thus, we tested whether the univalent MC associates with the XY body by X chromosome-specific FISH (Disteche and Adler, 1990) and an MC-specific alphoid probe. In 87–100% of late pachytene/diplotene monosomic nuclei ( $\geq 40$  nuclei analyzed in each of eight monosomic mice), the MC was associated with the morphologically distinct XY body. Furthermore,  $\sim 90\%$  of the MCs in disomic spermatocytes ( $\geq 29$  nuclei analyzed in each of two disomic mice) displayed an MC/sex body association. To scrutinize this association in more detail, we stained the MC by FISH and the sex-body chromatin with the XMR antibody (Calenda et al., 1994). 3D wide-field light microscopy disclosed that the MCs were located at the periphery or were partially submerged in the XMR-marked sex body (Fig. 5, A and B) in 97 and 94% of 35 monosomic and 34 disomic pachytene nuclei. Similar results were obtained when we stained the MC by FISH and the XY body with antibodies to phosphorylated histone ( $\gamma$ )H2ax (Fig. 5 C).  $\gamma$ -H2ax IF staining first marks the onset of DSB repair at meiosis, and later is restricted to the XY body, where it is required for meiotic sex chromosome inactivation (Mahadevaiah et al., 2001; Fernandez-Capetillo et al., 2003). At leptotene/zygotene, MCs were covered with the abundant  $\gamma$ -H2ax signals (unpublished data), whereas in pachytene nuclei, the  $\gamma$ -H2ax–sex body signal and MC signal partially colocalized (Fig. 5 C). However, monosomic and disomic MCs that were not associated with the XY body did not display a  $\gamma$ -H2ax signal (Fig. 5 D). This suggests that MCs likely follow the mode of DSB repair of their local chromatin environment.

Most interestingly, in 74% of disomic nuclei with an MC/sex body association both MC signals were paired (Fig. 5, B and C), whereas in the remaining 20% of the spermatocytes, the XY body-associated MCs were separated (Fig. 5 A). Localization of an MC completely inside the XY body was only seen in 3% of the nuclei analyzed, both in monosomic and disomic mice. Thus, it appears that the MC(s) undergoes an intimate interaction with the periphery of the XY body where it most likely “hitch-hikes” through male prophase I, thereby escaping potential checkpoints that control synapsis and/or DSB repair.

#### MC bivalents frequently disjoin precociously in MI, but maintain sister centromere cohesion

Next, we investigated, in disomic mice, whether an MC bivalent forms that aligns in the MI plate because disomic MCs in MI lacked the SCP3- and SCP1-positive “mini” cores as well as MLH1 foci at pachytene (unpublished data). This suggests that a fraction of MC bivalents may lack chiasmata and predicts that the MC bivalent could disjoin precociously.

MC FISH to MIs showed that only 18–44% of the disomic MIs ( $n = 23$ ; 28 and 9, respectively) contained paired MCs with juxtaposed FISH signals with their DAPI outline touching or overlapping (Fig. 6 A). The remaining disomic MIs

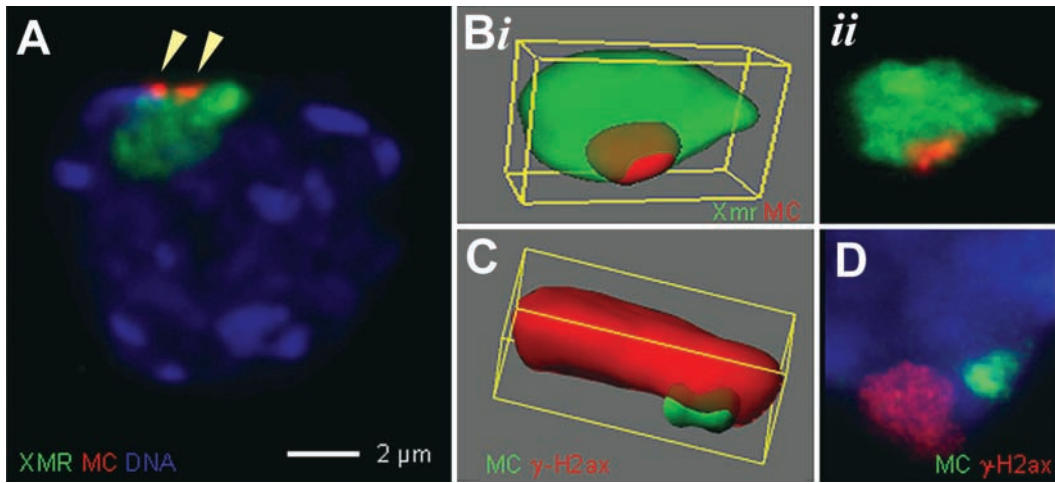


**Figure 5. MC/XY body associations as revealed by 3D imaging.** (A) Disomic pachytene nucleus ( $2MC^+-6$ ) shows the XY body (as defined by XMR IF staining, green) associated with two separated MCs (red signals,  $\alpha$ -satellite FISH; arrowheads). The image represents the projection of 10 optical sections encompassing the XY body as obtained by 3D imaging. Bar, 2  $\mu$ m. (B*i*) Deconvoluted 3D volume image from image planes encompassing an XY body from another disomic nucleus. The two paired MCs (one large red signal) are partially embedded (indicated by the shadowed part of the MC signal) in the XY body chromatin (green). (B*ii*) Shows a projection of the images before volume imaging. (C) Volume reconstruction of a  $\gamma$ -H2ax-stained XY body (red) and associated MCs (green). The paired MCs appear partially embedded in the XY chromatin. (D) Disomic spermatocyte (DNA blue; partial detail) showing the MC bivalent signal distant from the  $\gamma$ -H2ax-stained XY body (red). The paired MCs lack  $\gamma$ -H2ax signals.

contained separated MC signals (Fig. 6 B), which suggests that a significant number of MC bivalents separated precociously.

Next, we analyzed for sister chromatid cohesion by MC-specific PAC FISH, which creates minute FISH signals and allows to discriminate chromatid signals on MCs. Approxi-

mately 66% (mean; range 59–78%;  $n = 55$  MII nuclei) and 74% (mean; range 66–82%;  $n = 44$  MII nuclei) of the MCs in MII of respectively three monosomic and two disomic mice displayed two sister chromatid FISH signals (Fig. 6, C and D), which suggests that the MCs segregate to the same

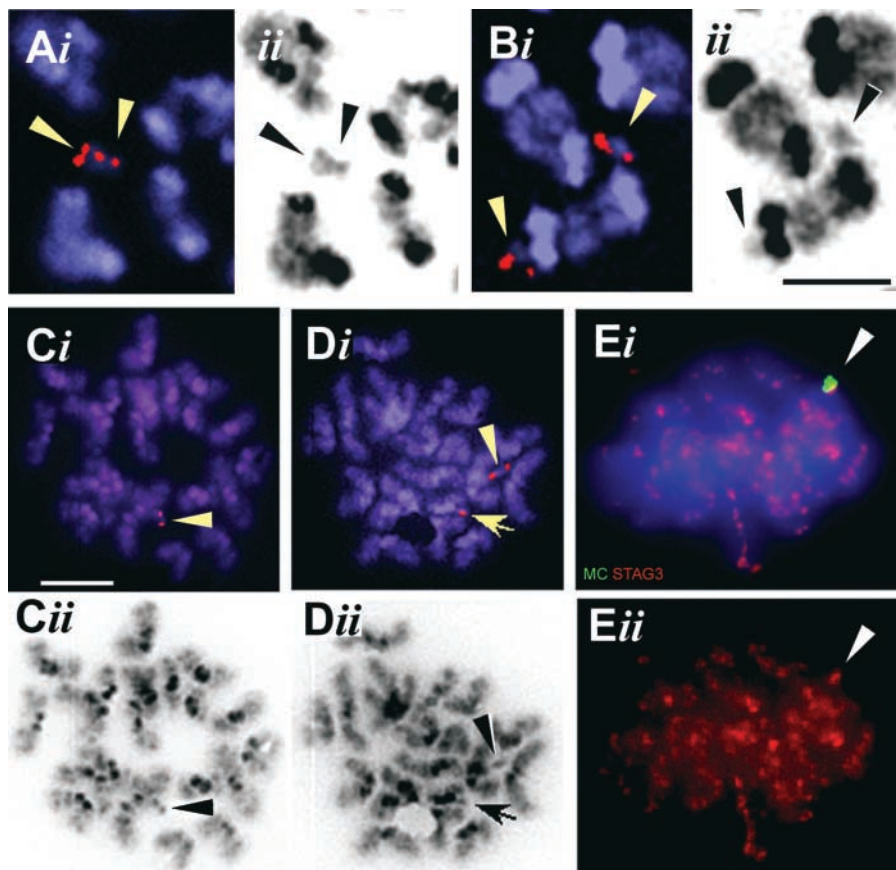


**Figure 6. MCs in MI and MII.** (A–D) FISH with an MC chromatid-specific PAC probe (red; see Materials and methods) on MI (A and B) and MII (C and D) spreads of a disomic mouse. (A*i*) An MC bivalent, remote from mouse centromeres, displays split FISH signals (arrowheads), indicating maintenance of cohesion at sister centromeres. (B*i*) Two MCs showing split chromatid signals (arrowheads) are located separate from each other, but each are associated with a mouse pericentric DAPI-bright heterochromatin block (black in *ii*). Bar, 5  $\mu$ m. (C*i*) An MC displaying sister chromatid signals (arrowhead) in an MII spermatocyte. Bar, 10  $\mu$ m. (D*i*) An MII spermatocyte with one MC with two chromatid signals (arrowhead) and a second MC that is present as a single sister chromatid (arrow) due to loss of sister chromatid cohesion during MI. All DAPI images (A*i*–D*ii*) are shown in grayscale. (E*i*) IF staining for STAG3 (red) combined with MC FISH (green) on a meiotic MI showing a STAG3 signal at the MC (arrowhead). (E*ii*) STAG3 channel only.

pole during anaphase I. In agreement with maintenance of sister centromere cohesion at MI, staining for the meiotic cohesin STAG3 revealed a dotlike signal at the MCs of both monosomic and disomic MI spermatocytes (Fig. 6 E).

### MCs can trigger the spindle checkpoint

Homologous centromeres that fail to attach to opposite spindle poles, and hence the lack of tension during MI, may

trigger the spindle assembly checkpoint in MI (Rieder et al., 1995; Woods et al., 1999; Shonn et al., 2000; Nicklas et al., 2001). Thus, we determined that in the behavior of MCs during mouse MI and MII in stage XII tubules of monosomic, disomic, and wild-type testes sections by TUNEL labeling and anti-phosphohistone H3 (pH3; a metaphase marker) immunofluorescence, meiotic divisions occur only at this stage of mouse spermatogenesis (Oakberg, 1956). In-

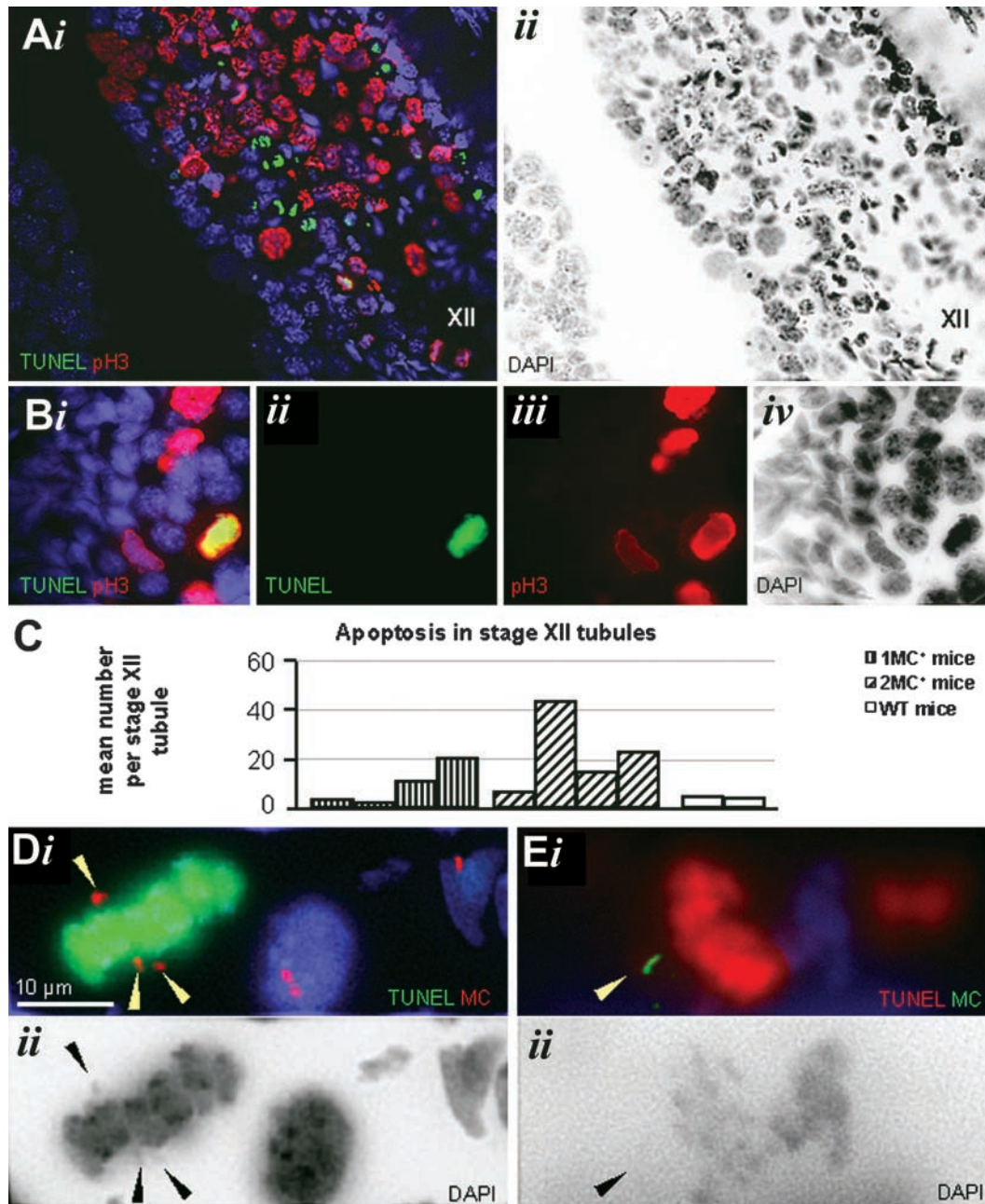


**Figure 7. Metaphase checkpoint response in monosomic and disomic MC<sup>+</sup> spermatogenesis.** (A and B) IF staining for phosphohistone H3 (pH3, red signal) combined with TUNEL labeling (green) on frozen testes sections of a disomic mouse. XII denotes a part of a seminiferous tubule at stage XII. (B) An apoptotic metaphase positive for TUNEL (green) and pH3 labeling (red); (ii) green channel, (iii) red channel, (iv) color inverted, grayscale DAPI image. (C) Table of the mean number of apoptotic nuclei detected in stage XII tubules of two WT, four monosomic (1MC<sup>+</sup>-64, -66, -73 and -7), and four disomic testes (2MC<sup>+</sup>-4, -6, -13 and -16). Apoptotic cell death of metaphase cells ( $\geq 70\%$  of all apoptotic cells) was increased in disomic as well as monosomic MC<sup>+</sup> spermatogenesis. (D) TUNEL-labeled (green) apoptotic MI that displays a precociously separated MC bivalent (red, arrowheads). One homologue has lost sister cohesion (bottom arrowheads). (E) TUNEL-positive apoptotic MI (red) with an MC (arrowhead) off the MI plate. (Aii, Bii, Dii, and Eii) Corresponding, color-inverted, grayscale DAPI images.

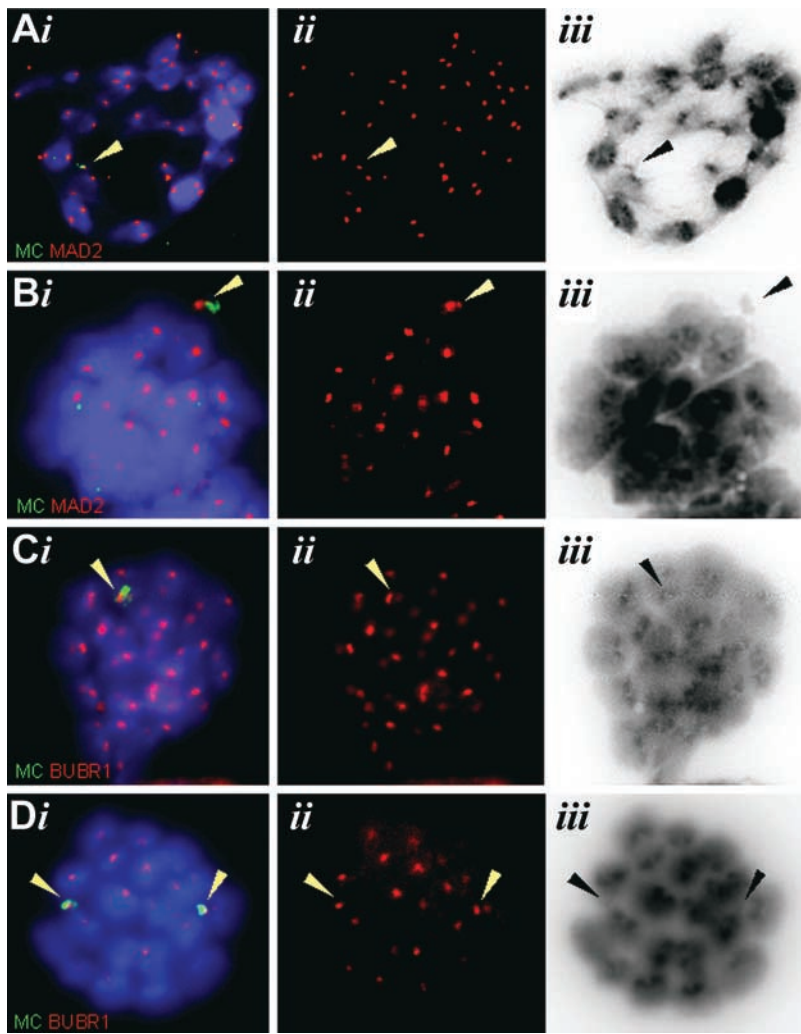


Figure 8. **MAD2 and BUBR1 staining of (pro-)metaphases I and II.** (A*i*) IF staining for MAD2 (red) combined with MC-FISH (green) on a meiotic prometaphase I reveals presence of MAD2 at the MC kinetochores. (B*i*) Meiotic prometaphase II with MAD2 present at the MC kinetochores. (C*i*) Presence of BUBR1 signals (red) and MC-FISH signals in a prometaphase I. (D*i*) Meiotic prometaphase II with BUBR1 detected at the MC kinetochores. Arrowheads denote the MC FISH signals (*i*) and their respective kinetochores signals (*ii*). (A*ii*–D*ii*) Red channels only. (A*iii*–D*iii*) Corresponding color-inverted, grayscale DAPI images.

investigation of >10 stage XII tubule cross sections per testis of each of four monosomic, four disomic, and two wild-type testes revealed a 2–10-fold increase in the mean number of apoptotic cells in monosomic and disomic MC-containing stage XII tubules when compared with wild-type stage XII tubules (Fig. 7 C), with  $\geq 70\%$  of the apoptotic cells being metaphases (Fig. 7, A and B). Furthermore, apoptotic MIs generally revealed one or more MC signals off the MI plate (Fig. 7, D and E), which suggests that precocious separation of MC bivalents and/or noncongressed MCs triggered the spindle checkpoint. In agreement, it was found that MC kinetochores in prometaphase I and II spermatocytes displayed distinct signals of MAD2 (Chen et al., 1996) and BUBR1 (Chan et al., 1998; Fig. 8, A–D), proteins that are central to the spindle checkpoint (Cleveland et al., 2003).

#### MCs associate with pericentric heterochromatin at MI

However, the question remained how the majority of mono- and disomic MCs bypass the meiotic spindle checkpoint and are transmitted to the offspring. Univalent human mini- or microchromosomes have been reported to pass through the germ line and show an inherent tendency for centromeric associations (Felbor et al., 2002). Because heterochromatin associations have the capacity to perpetuate the segregation of nonexchange chromosomes in some organisms (for re-

view see McKim and Hawley, 1995; Bernard and Allshire, 2002), we determined whether our MC(s) undergo associations with mouse pericentromeric heterochromatin by MC-specific  $\alpha$ -satellite and mouse major satellite DNA FISH to MIs. About 60% of the MCs of monosomic mice showed associations between the MC and the pericentric heterochromatin of MI bivalents (Fig. 9 A). A high frequency of MC–heterochromatin association was also seen in disomic MC spermatocytes (Fig. 9 B). Thus, it may be assumed that centromeric associations, possibly instigated by the general stickiness of pericentric heterochromatin earlier during mouse prophase I (Hsu et al., 1971; Scherthan et al., 1996), may contribute to transmission of MCs through the mammalian germ line.

#### Discussion

We have investigated the transmission of one or more circular MC during mammalian spermatogenesis. These MCs contain human  $\alpha$ -satellite and unique DNA sequences, and assemble functional centromeres that contain kinetochores that are associated with spindle checkpoint proteins like MAD2 (Chen et al., 1996) and BUBR1 (Chan et al., 1998), whereas MCs lack telomere sequences (Voet et al., 2001) and associated proteins.

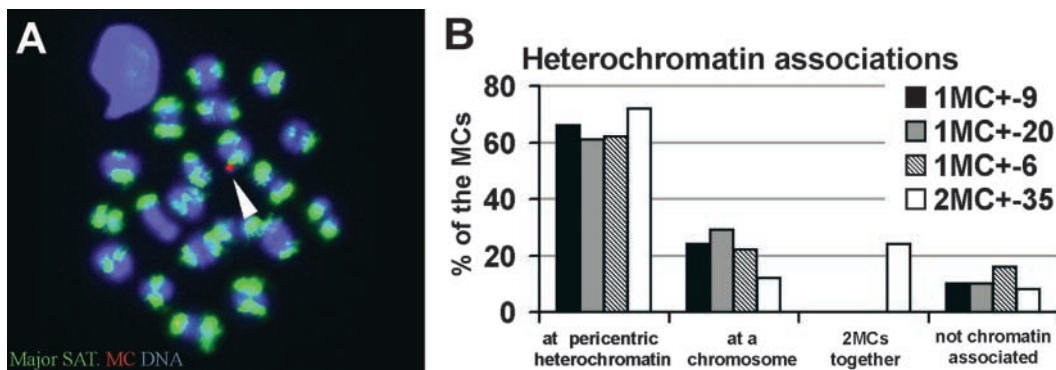


Figure 9. **Heterochromatin associations of MCs in MI.** (A) Mouse major satellite DNA FISH (green) and  $\alpha$ -satellite DNA MC-FISH (red) on an MI spread shows the MC signal touching the pericentric heterochromatin of a mouse bivalent (arrowhead). (B) Frequencies of MC associations with mouse pericentromeric heterochromatin during the first meiotic metaphase. All mice used, except mouse 2MC<sup>+</sup>-35, are monosomic MC<sup>+</sup> mice. In the MI spermatocytes of mouse 2MC<sup>+</sup>-35, a total of 25 MCs was scored (nine nuclei with one MC; eight nuclei with two MCs). 8% of these MCs were located together and were also associated with pericentric heterochromatin (number implemented in both bars). Another 8% of the MCs localized next to each other and to the euchromatic part of a mouse chromosome (number implemented in both bars).

### Telomere-independent homologue pairing of MCs

The unique MC<sup>+</sup> karyotype allowed for the first time to test the requirement of telomeres for participating in meiotic telomere clustering (bouquet formation) and its contribution to the meiotic homologue pairing process in mammals. MCs without telomeres generally located remote from the telomere cluster in the majority of monosomic and disomic bouquet nuclei. The occasional association of a circular MC at the bouquet basis could be a consequence of MC–heterochromatin associations during mouse prophase I. Thus, our data provide evidence that telomeres are required for participation in the mammalian bouquet stage. They contrast with the association of a plant ring chromosome with the telomere cluster in the maize bouquet (Carlton and Cande, 2002), and suggest that the latter is mediated by a significant amount of interstitial telomere sequences still present at the fusion site of the maize ring chromosome. The findings in mammalian MC<sup>+</sup> meiosis are in agreement with those in *Schizosaccharomyces pombe* meiosis, where functional telomeres are required for bouquet formation and the tethering of an MC to the bouquet base (for review see Yamamoto and Hiraoka, 2001). Thus, it will be interesting to investigate the behavior of telomere-bearing MCs in mammalian meiosis.

Due to the above features, we expected that the MC homologues would fail to pair. Surprisingly, a high number of the disomic pachytene nuclei displayed paired MCs that were connected by short SCP1-positive structures, which indicates a telomere-independent pathway to homologue pairing—at least for small mammalian supernumerary chromosomes. Surprisingly, in both monosomic and disomic spermatocytes, the MC(s) located to the periphery of the XY body. Notwithstanding other possibilities, it seems likely that passive movements of MCs, induced by the general nuclear and chromosome movements that occur during leptotene/zygotene of mammalian prophase I (Parvinen and Soderstrom, 1976; Scherthan et al., 1996), may have led to the association of the MCs with each other and the XY body. The possibility that somatic MC associations may have contributed to this meiotic pairing is unlikely because MC signals were spatially separated in the majority of premeiotic cells, a distribution that

reflects homologue separation in most mammalian spermatogonia (Scherthan et al., 1996; Pfeifer et al., 2001).

### MCs pass the pachytene checkpoint

Analyses in knockout mice and yeasts have provided evidence for tight control of meiotic prophase progression (Roeder and Bailis, 2000). Pachytene checkpoint control likely monitors timely completion of DSB repair and chromosome synapsis, and elicits apoptotic cell death in male mice if triggered by the presence of unpaired axial cores (Odorisio et al., 1998; Cohen and Pollard, 2001). Surprisingly, similar amounts of apoptotic cell death in stage I–XI testes tubules and similar testis weights of MC<sup>+</sup> and wild-type mice indicate that the MCs bypass these surveillance mechanisms at prophase I. This is likely mediated by assembly of a small meiotic chromosome core on the MC that contains meiosis-specific cohesins SCP3 and SCP1. The presence of SCP1 on univalent MCs suggests that these undergo self-synapsis. Self-synapsis occurs at univalent X chromosomes in female XO mice (Speed, 1986) and at unpaired XY axes (Eaker et al., 2001), and perpetuates meiosis in the haploid condition (Levan, 1942; Loidl et al., 1991). In the disomic condition, short SCP1-staining cores connected MC homologues, suggesting an authentic mode of synapsis.

Furthermore, the association of MC(s) with the XY body may mask any unpaired AEs from surveillance mechanisms because it tolerates the presence of unpaired chromosome axes (Jablonka and Lamb, 1988). The association of monosomic and disomic MCs with the sex body may thus be a crucial feature for their transmission through the male germ line and may explain the absence of fertility problems in the MC<sup>+</sup> mice. In agreement, passage of a supernumerary chromosome 21 up to MI was most likely mediated by XY body association (Johannisson et al., 1983).

### MCs and the spindle checkpoint

The spindle checkpoint in male mammalian meiosis I (LeMaire-Adkins et al., 1997) is triggered by kinetochores that are not under tension (Eaker et al., 2001; Skoufias et al.,

2001). During meiosis I, chiasmata contribute to the formation of tension at bivalents (Rieder et al., 1995; Shonn et al., 2000; Nicklas et al., 2001; for review see Petronczki et al., 2003). Mammalian univalent chromosomes have been found to trigger the spindle assembly checkpoint leading to apoptotic cell death of MI spermatocytes (Eaker et al., 2001, 2002). MAD2 and BUBR1, proteins whose turnover is crucial for spindle checkpoint function (Skoufias et al., 2001; Cleveland et al., 2003), both were present at MC kinetochores, suggesting that MCs are subject to checkpoint control. In agreement, disomic MCs that had separated precociously triggered apoptosis of metaphase cells. Similarly, univalent (monosomic) MCs were also able to trigger the spindle checkpoint. However, most univalent MCs maintained centromere cohesion and segregated randomly in the MI division, thus undergoing a mode of segregation that has been observed for univalent chromosomes in grasshopper meiosis (Rebollo and Arana, 1998).

### MCs associate with pericentric heterochromatin

Despite spindle checkpoint activation in some MC<sup>+</sup> metaphase spermatocytes, a large number of MCs were present in mature sperm, suggesting a bypass to spindle checkpoint control. Heterochromatin associations have the potential to compensate for absence of chiasmata and perpetuate the segregation of nonexchange chromosomes in flies (Dernburg et al., 1996). In MC<sup>+</sup> MIs, we noted a frequent association of the MCs with the pericentromeric heterochromatin of mouse MI chromosomes. Moreover, human microchromosomes that showed centromeric associations at metaphase have been transmitted through the germ line (Felbor et al., 2002). Therefore, and because MCs consist largely of satellite DNA, a building block of heterochromatin, it may be speculated that such associations could provide for a physical tether that compensates for the absence of a homologue, thereby allowing for bypass of the spindle checkpoint in male meiosis.

Altogether, our current data disclose a telomere-independent MC homologue-pairing mechanism and the existence of important escape routes to meiotic checkpoint control, both in prophase I and meiotic divisions. Such bypasses may underlie the efficient germ line transmission of human MCs and the generation of aneuploid sperm in healthy human males.

## Materials and methods

### Mice

Mice containing the MC were generated as described previously (Voet et al., 2001). In brief, we generated two male chimeras containing a chromosomal vector (MC) by standard blastocyst injection of MC<sup>+</sup> embryonic stem cells. These chimeras were mated with C57Bl/6 wild-type mice. Starting from monosomic F1-1MC<sup>+</sup> mice, the MC was further bred into the C57Bl/6 and NMRI genetic background. The F3 and F4 inbreeds were used for meiotic analyses. For the generation of disomic mice, monosomic and disomic mice were respectively mated with each other.

### Testicular specimens

Adult and 12-d post partum male mice were killed by cervical dislocation, and testes were immediately resected and processed. For generating frozen testes sections and IF staining, testes were shock frozen for 5 min in 2-methyl-butane at  $-70^{\circ}\text{C}$  and stored at  $-70^{\circ}\text{C}$  until further use (Scherthan, 2002).

### Testicular preparations

Preparations for simultaneous IF staining and FISH were prepared by generating 14- $\mu\text{m}$  frozen testes sections or by a modified squash procedure (Page et al., 1998). In brief, frozen testicular tissue was minced in hypotonic solution (0.075 M KCl) at RT. A drop of the suspension was placed on clean aminosilane-coated glass slides and immediately mixed with two drops of fixative (3.7% formaldehyde, pH 7.4). A coverslip was placed on top of the suspension and pressure was applied. Slides with coverslip were submerged in liquid nitrogen. After freezing, the coverslip was removed and preparations were subjected to IF staining as described later in Materials and methods. Meiotic chromosome spreads were prepared as described by Evans (1979).

Detergent spreading of spermatocytes was performed as described previously (Peters et al., 1997; Scherthan et al., 2000) with modifications as follows:  $\sim 10\ \mu\text{l}$  of a testicular suspension was placed on a glass slide and mixed gently with 80  $\mu\text{l}$  ionic detergent solution 1% Lipsol (LIP Equipment). After 5 min, cells were mixed with 1% PFA, 5 mM NaBH<sub>3</sub>, pH 9.2, and 0.15% Triton X-100, and slowly dried in a humid chamber for 2 h, washed 3 $\times$  with 0.01% Agepon (Agfa), and stored at  $-70^{\circ}\text{C}$  until further use.

### DNA probes

The  $\alpha$ -satellite DNA probe was generated by low stringency PCR using primers (5'-AGTAAGTTCTTTGTGTTGCCTC-3'; 5'-CAGAGTGTTC-CAAACACTCTATG-3') and as template DNA of an MC<sup>+</sup> hamster cell line (Voet et al., 2001). The mouse major satellite DNA probe was prepared by PCR using mouse genomic DNA as template and primers (5'-CCTG-GAATATGGCGAGAAAA-3'; 5'-TCGTCATTTTCAAGTCGTCA-3'; Scherthan et al., 1996). The probe for the repeat cluster near the centromere of the X chromosome (DXWas70; Disteche and Adler, 1990) was a gift of C. Disteche (University of Washington, Seattle, WA). P1 artificial chromosomes (RP5-837O21 and RP5-573H3) were used as probes for detecting human chromosome 1p sequences on the MC.

### Antisera

Antisera to SC proteins SCP3 (Lammers et al., 1994) and SCP1 (Meuwissen et al., 1992) were gifts of C. Heyting (Wageningen University, Wageningen, Netherlands); anti-STAG3 (Pezzi et al., 2000) was a gift of J. Barbero (Universidad Autónoma de Madrid, Madrid, Spain); anti-MAD2 (Chen et al., 1996) was a gift of R.H. Chen (Cornell University, Ithaca, NY); anti-hBUBR1 (Chan et al., 1998) was a gift from T.J. Yen (Fox Chase Cancer Center, Philadelphia, PA); anti-XMR (Calenda et al., 1994) was a gift from H. Garchon (INSERM U25, Paris, France); and anti-CENP-C was a gift from W.C. Earnshaw (University of Edinburgh, Edinburgh, UK). Anti-M31 was from Serotec; anti-phosphorylated histone H3 was from New England Biolabs, Inc.; and anti-MLH1 was from BD Biosciences; anti- $\gamma$ -H2ax was from Upstate Biotechnology. Anti-TRF1 and anti-hRAP1 antibodies (Broccoli et al., 1997; Li et al., 2000) were gifts of T. de Lange (The Rockefeller University, NY). CREST antiserum was as described previously (Scherthan, 1995).

### Immunofluorescence

Frozen testes sections were cut on a cryostat (Microm) and immediately fixed with 1% PFA/PBS for 10 min. After two 10-min washes in PBS, 0.2% Triton X-100/PBS/0.5% blocking reagent (Roche) was applied for 1 h. Antibody solution (in 0.5% blocking reagent/PBS) was left on the slides overnight at 4 $^{\circ}\text{C}$ . Next, the slides were washed 3 $\times$  and detection was performed with a fluorescently labeled secondary antibody (Vector Laboratories). After three 10-min washes in PBS, the signal was fixed with 1% PFA/PBS for 5 min followed by a PBS wash and FISH. A similar protocol was used for IF staining on the squashed cells, leaving out the first fixation step. Spread meiotic cells were obtained, FISHed, and immunostained as described previously (Scherthan, 2002).

### FISH

Probes were labeled with digoxigenin-11-dUTP using the DIG-Nick Translation Mix (Roche), or with either biotin-16-dUTP, fluorescein-12-dUTP (Invitrogen), or lissamine-5-dUTP (Dupont) using the Nick Translation System (Invitrogen). The FISH procedure and fluorescent detection was performed as described previously (Voet et al., 2001). FISH with a FITC-(C<sub>3</sub>TA<sub>2</sub>)<sub>3</sub> PNA probe was performed as described previously (Vermeesch et al., 1998). In some experiments, a conventional telomere repeat probe was applied (Scherthan, 2002). Finally, DNA was counterstained with DAPI and the slides mounted in Vectashield<sup>®</sup> (Vector Laboratories). FISH on sperm was performed as described by Kobayashi et al. (1999).

**Apoptosis assay**

Apoptotic cells in testes tissue sections and suspensions were labeled using a TUNEL assay (Roche) according to instructions of the supplier.

**Light microscopic evaluation and image recording**

Preparations were evaluated using an epi-fluorescence microscope (Leica). Digital images were recorded with a CCD camera (Photometrics) using the QlipsFISH system (Vysis) or the ISIS fluorescence image analysis system (MetaSystems).

3D evaluation of protein axes and MC colocalization was performed using an epi-fluorescence microscope (Axioskop; Carl Zeiss MicroImaging, Inc.) equipped with a 100× plan-neofluar oil-immersion lens (NA 1.35; Carl Zeiss MicroImaging, Inc.) attached to a PIFOC z-SCAN (Physik Instrumente), and a 12-bit CCD digital camera (SensiCam; PCO) controlled by TILLvisION v4.0 software. Fluorochromes were excited using a polychrome IV monochromator (T.I.L.L. Photonics) in combination with a quadruple band pass beam splitter and barrier filter (Chroma Technology Corp.) allowing subsequent recording of blue (DAPI), red (Cy3), green (FITC), and infrared (Cy5) fluorescence for the same focal plane. Spatial relationship of protein signals and MC signal was also determined by interactively scanning through the image stacks. Deconvolution was performed using the cMLE algorithm of Huygens 2.1.4-essential (Scientific Volume Imaging) running under Windows NT. Rendering of 3D data was done using the Surpass module of Imaris 3.3.2 (Bitplane).

We are grateful to C. Heyting, H.J. Garchon (Hopital Necker, Paris, France), W.C. Earnshaw, J.L. Barbero, T. de Lange, and R.H. Chen for support with the antibodies. We thank C. Disteche for the X probe and E. Legius for statistical advice.

H. Scherthan acknowledges support from the Deutsche Forschungsgemeinschaft (grant SCHE 350/8-4) and H.H. Ropers, (Max-Planck-Institute for Molecular Genetics, Berlin, Germany). T. Voet was supported by a scholarship of the Institute for the Promotion of Innovation by Science and Technology in Flanders (IWT). The authors confirm that there are no conflicting interests.

Submitted: 14 May 2003

Accepted: 7 July 2003

**References**

Bernard, P., and R. Allshire. 2002. Centromeres become unstuck without heterochromatin. *Trends Cell Biol.* 12:419–424.

Broccoli, D., L. Chong, S. Oelmann, A.A. Fernald, N. Marziliano, B. van Steensel, D. Kipling, M.M. Le Beau, and T. de Lange. 1997. Comparison of the human and mouse genes encoding the telomeric protein, TRF1: chromosomal localization, expression and conserved protein domains. *Hum. Mol. Genet.* 6:69–76.

Buonomo, S.B., R.K. Clyne, J. Fuchs, J. Loidl, F. Uhlmann, and K. Nasmyth. 2000. Disjunction of homologous chromosomes in meiosis I depends on proteolytic cleavage of the meiotic cohesin Rec8 by separin. *Cell.* 103:387–398.

Calenda, A., B. Allenet, D. Escalier, and J.F. Bach. 1994. The meiosis-specific Xmr gene product is homologous to the lymphocyte Xlr protein and is a component of the XY body. *EMBO J.* 13:100–109.

Carlton, P.M., and W.Z. Cande. 2002. Telomeres act autonomously in maize to organize the meiotic bouquet from a semipolarized chromosome orientation. *J. Cell Biol.* 157:231–242.

Chan, G.K., B.T. Schaar, and T.J. Yen. 1998. Characterization of the kinetochore binding domain of CENP-E reveals interactions with the kinetochore proteins CENP-F and hBUBR1. *J. Cell Biol.* 143:49–63.

Chen, R.H., J.C. Waters, E.D. Salmon, and A.W. Murray. 1996. Association of spindle assembly checkpoint component XMad2 with unattached kinetochores. *Science.* 274:242–246.

Cleveland, D.W., Y. Mao, and K.F. Sullivan. 2003. Centromeres and kinetochores: from epigenetics to mitotic checkpoint signaling. *Cell.* 112:407–421.

Cohen, P.E., and J.W. Pollard. 2001. Regulation of meiotic recombination and prophase I progression in mammals. *Bioessays.* 23:996–1009.

Dernburg, A.F., J.W. Sedat, and R.S. Hawley. 1996. Direct evidence of a role for heterochromatin in meiotic chromosome segregation. *Cell.* 86:135–146.

Disteche, C.M., and D.A. Adler. 1990. Localization of a mouse centromeric DNA repeat in interphase nuclei. *Cytometry.* 11:119–125.

Dobson, M.J., R.E. Pearlman, A. Karaiskakis, B. Spyropoulos, and P.B. Moens.

1994. Synaptonemal complex proteins: occurrence, epitope mapping and chromosome disjunction. *J. Cell Sci.* 107:2749–2760.

Eaker, S., A. Pyle, J. Cobb, and M.A. Handel. 2001. Evidence for meiotic spindle checkpoint from analysis of spermatocytes from Robertsonian-chromosome heterozygous mice. *J. Cell Sci.* 114:2953–2965.

Eaker, S., J. Cobb, A. Pyle, and M.A. Handel. 2002. Meiotic prophase abnormalities and metaphase cell death in MLH1-deficient mouse spermatocytes: insights into regulation of spermatogenic progress. *Dev. Biol.* 249:85–95.

Eijpe, M., H. Offenberger, R. Jessberger, E. Revenkova, and C. Heyting. 2003. Meiotic cohesin REC8 marks the axial elements of rat synaptonemal complexes before cohesins SMC1beta and SMC3. *J. Cell Biol.* 160:657–670.

Escalier, D. 2001. Impact of genetic engineering on the understanding of spermatogenesis. *Hum. Reprod. Update.* 7:191–210.

Evans, E.P. 1979. Cytological methods for the study of meiotic properties in mice. *Genetics.* 92:s97–s103.

Felbor, U., D. Rutschow, T. Haaf, and M. Schmid. 2002. Centromeric association of chromosome 16- and 18-derived microchromosomes. *Hum. Genet.* 111:16–25.

Fernandez-Capetillo, O., S.K. Mahadevaiah, A. Celeste, P.J. Romanienko, R.D. Camerini-Otero, W.M. Bonner, K. Manova, P. Burgoyne, and A. Nussenzweig. 2003. H2AX is required for chromatin remodeling and inactivation of sex chromosomes in male mouse meiosis. *Dev. Cell.* 4:497–508.

Hsu, T.C., J.E. Cooper, M.L. Mace, Jr., and B.R. Brinkley. 1971. Arrangement of centromeres in mouse cells. *Chromosoma.* 34:73–87.

Hunt, P.A., and T.J. Hassold. 2002. Sex matters in meiosis. *Science.* 296:2181–2183.

Jablonka, E., and M.J. Lamb. 1988. Meiotic pairing constraints and the activity of sex chromosomes. *J. Theor. Biol.* 133:23–36.

Johannisson, R., A. Gropp, H. Winking, W. Coerd, H. Rehder, and E. Schwinger. 1983. Down's syndrome in the male. Reproductive pathology and meiotic studies. *Hum. Genet.* 63:132–138.

Kobayashi, J., T. Kohsaka, H. Sasada, M. Umez, and E. Sato. 1999. Fluorescence in situ hybridization with Y chromosome-specific probe in decondensed bovine spermatozoa. *Theriogenology.* 52:1043–1054.

Lammers, J.H., H.H. Offenberger, M. van Aalderen, A.C. Vink, A.J. Dietrich, and C. Heyting. 1994. The gene encoding a major component of the lateral elements of synaptonemal complexes of the rat is related to X-linked lymphocyte-regulated genes. *Mol. Cell Biol.* 14:1137–1146.

LeMaire-Adkins, R., K. Radke, and P.A. Hunt. 1997. Lack of checkpoint control at the metaphase/anaphase transition: a mechanism of meiotic nondisjunction in mammalian females. *J. Cell Biol.* 139:1611–1619.

Levan, A. 1942. Studies on the mechanism of haploid rye. *Hereditas.* 28:177–211.

Li, B., S. Oestreich, and T. de Lange. 2000. Identification of human Rap1: implications for telomere evolution. *Cell.* 101:471–483.

Loidl, J., K. Nairz, and F. Klein. 1991. Meiotic chromosome synapsis in a haploid yeast. *Chromosoma.* 100:221–228.

Mahadevaiah, S.K., J.M. Turner, F. Baudat, E.P. Rogakou, P. de Boer, J. Blanco-Rodriguez, M. Jasin, S. Keeney, W.M. Bonner, and P.S. Burgoyne. 2001. Recombinational DNA double-strand breaks in mice precede synapsis. *Nat. Genet.* 27:271–276.

McKim, K.S., and R.S. Hawley. 1995. Chromosomal control of meiotic cell division. *Science.* 270:1595–1601.

Meuwissen, R.L., H.H. Offenberger, A.J. Dietrich, A. Riesewijk, M. van Iersel, and C. Heyting. 1992. A coiled-coil related protein specific for synapsed regions of meiotic prophase chromosomes. *EMBO J.* 11:5091–5100.

Nicklas, R.B., J.C. Waters, E.D. Salmon, and S.C. Ward. 2001. Checkpoint signals in grasshopper meiosis are sensitive to microtubule attachment, but tension is still essential. *J. Cell Sci.* 114:4173–4183.

Oakberg, E.F. 1956. A description of spermatogenesis in the mouse and its use in analysis of the cycle of the seminiferous epithelium and germ cell renewal. *Am. J. Anat.* 99:391–413.

Odoriso, T., T.A. Rodriguez, E.P. Evans, A.R. Clarke, and P.S. Burgoyne. 1998. The meiotic checkpoint monitoring synapsis eliminates spermatocytes via p53-independent apoptosis. *Nat. Genet.* 18:257–261.

Offenberger, H.H., J.A. Schalk, R.L. Meuwissen, M. van Aalderen, H.A. Kester, A.J. Dietrich, and C. Heyting. 1998. SCP2: a major protein component of the axial elements of synaptonemal complexes of the rat. *Nucleic Acids Res.* 26:2572–2579.

Page, J., J.A. Suja, J.L. Santos, and J.S. Rufas. 1998. Squash procedure for protein immunolocalization in meiotic cells. *Chromosome Res.* 6:639–642.

Parvinen, M., and K.O. Soderstrom. 1976. Chromosome rotation and formation of synapsis. *Nature.* 260:534–535.

- Pelttari, J., M.R. Hoja, L. Yuan, J.G. Liu, E. Brundell, P. Moens, S. Santucci-Darmanin, R. Jessberger, J.L. Barbero, C. Heyting, and C. Hoog. 2001. A meiotic chromosomal core consisting of cohesin complex proteins recruits DNA recombination proteins and promotes synapsis in the absence of an axial element in mammalian meiotic cells. *Mol. Cell. Biol.* 21:5667–5677.
- Peters, A.H., A.W. Plug, M.J. van Vugt, and P. de Boer. 1997. A drying-down technique for the spreading of mammalian meiocytes from the male and female germline. *Chromosome Res.* 5:66–68.
- Petronczki, M., M.F. Siomos, and K. Nasmyth. 2003. Un menage a quatre: the molecular biology of chromosome segregation in meiosis. *Cell.* 112:423–440.
- Pezzi, N., I. Prieto, L. Kremer, L.A. Perez Jurado, C. Valero, J. del Mazo, A. Martinez, and J.L. Barbero. 2000. STAG3, a novel gene encoding a protein involved in meiotic chromosome pairing and location of STAG3-related genes flanking the Williams-Beuren syndrome deletion. *FASEB J.* 14:581–592.
- Pfeifer, C., P.D. Thomsen, and H. Scherthan. 2001. Centromere and telomere redistribution precedes homologue pairing and terminal synapsis initiation during prophase I of cattle spermatogenesis. *Cytogenet. Cell Genet.* 93:304–314.
- Prieto, I., J.A. Suja, N. Pezzi, L. Kremer, A. Martinez, J.S. Rufas, and J.L. Barbero. 2001. Mammalian STAG3 is a cohesin specific to sister chromatid arms in meiosis I. *Nat. Cell Biol.* 3:761–766.
- Prieto, I., N. Pezzi, J.M. Buesa, L. Kremer, I. Barthelemy, C. Carreiro, F. Roncal, A. Martinez, L. Gomez, R. Fernandez, et al. 2002. STAG2 and Rad21 mammalian mitotic cohesins are implicated in meiosis. *EMBO Rep.* 3:543–550.
- Rebollo, E., and P. Arana. 1998. Chromosomal factors affecting the transmission of univalents. *Chromosome Res.* 6:67–69.
- Revenkova, E., M. Eijpe, C. Heyting, B. Gross, and R. Jessberger. 2001. Novel meiosis-specific isoform of mammalian SMC1. *Mol. Cell. Biol.* 21:6984–6998.
- Rieder, C.L., R.W. Cole, A. Khodjakov, and G. Sluder. 1995. The checkpoint delaying anaphase in response to chromosome monoorientation is mediated by an inhibitory signal produced by unattached kinetochores. *J. Cell Biol.* 130:941–948.
- Roeder, G.S., and J.M. Bailis. 2000. The pachytene checkpoint. *Trends Genet.* 16:395–403.
- Schalk, J.A., A.J. Dietrich, A.C. Vink, H.H. Offenberg, M. van Aalderen, and C. Heyting. 1998. Localization of SCP2 and SCP3 protein molecules within synaptonemal complexes of the rat. *Chromosoma.* 107:540–548.
- Scherthan, H. 1995. Chromosome evolution in muntjac revealed by centromere, telomere and whole chromosome paint probes. In Kew Chromosome Conference IV. P.E. Brandham and M.D. Bennett, editors. Royal Botanic Gardens, Kew. 267–280.
- Scherthan, H. 2001. A bouquet makes ends meet. *Nat. Rev. Mol. Cell Biol.* 2:621–627.
- Scherthan, H. 2002. Detection of chromosome ends by telomere FISH. *Methods Mol. Biol.* 191:13–31.
- Scherthan, H., S. Weich, H. Schwegler, C. Heyting, M. Harle, and T. Cremer. 1996. Centromere and telomere movements during early meiotic prophase of mouse and man are associated with the onset of chromosome pairing. *J. Cell Biol.* 134:1109–1125.
- Scherthan, H., M. Jerratsch, B. Li, S. Smith, M. Hulten, T. Lock, and T. de Lange. 2000. Mammalian meiotic telomeres: protein composition and redistribution in relation to nuclear pores. *Mol. Biol. Cell.* 11:4189–4203.
- Schmekel, K., R.L. Meuwissen, A.J. Dietrich, A.C. Vink, J. van Marle, H. van Veen, and C. Heyting. 1996. Organization of SCP1 protein molecules within synaptonemal complexes of the rat. *Exp. Cell Res.* 226:20–30.
- Shonn, M.A., R. McCarroll, and A.W. Murray. 2000. Requirement of the spindle checkpoint for proper chromosome segregation in budding yeast meiosis. *Science.* 289:300–303.
- Skoufias, D.A., P.R. Andreassen, F.B. Lacroix, L. Wilson, and R.L. Margolis. 2001. Mammalian mad2 and bub1/bubR1 recognize distinct spindle-attachment and kinetochore-tension checkpoints. *Proc. Natl. Acad. Sci. USA.* 98:4492–4497.
- Sluder, G., and D. McCollum. 2000. Molecular biology. The mad ways of meiosis. *Science.* 289:254–255.
- Speed, R.M. 1986. Oocyte development in XO fetuses of man and mouse: the possible role of heterologous X-chromosome pairing in germ cell survival. *Chromosoma.* 94:115–124.
- Turner, J.M., S.K. Mahadevaiah, R. Benavente, H.H. Offenberg, C. Heyting, and P.S. Burgoyne. 2000. Analysis of male meiotic “sex body” proteins during XY female meiosis provides new insights into their functions. *Chromosoma.* 109:426–432.
- Vermeesch, J.R., D. Falzetti, G. Van Buggenhout, J.P. Fryns, and P. Marynen. 1998. Chromosome healing of constitutional chromosome deletions studied by microdissection. *Cytogenet. Cell Genet.* 81:68–72.
- Voet, T., J. Vermeesch, A. Carens, J. Durr, C. Labaere, H. Duhamel, G. David, and P. Marynen. 2001. Efficient male and female germline transmission of a human chromosomal vector in mice. *Genome Res.* 11:124–136.
- Voet, T., E. Schoenmakers, S. Carpentier, C. Labaere, and P. Marynen. 2003. Controlled transgene dosage and PAC mediated transgenesis in mice using a chromosomal vector. *Genomics.* In press.
- von Wettstein, D., S.W. Rasmussen, and P.B. Holm. 1984. The synaptonemal complex in genetic segregation. *Annu. Rev. Genet.* 18:331–413.
- Woods, L.M., C.A. Hodges, E. Baart, S.M. Baker, M. Liskay, and P.A. Hunt. 1999. Chromosomal influence on meiotic spindle assembly: abnormal meiosis I in female Mlh1 mutant mice. *J. Cell Biol.* 145:1395–1406.
- Yamamoto, A., and Y. Hiraoka. 2001. How do meiotic chromosomes meet their homologous partners?: lessons from fission yeast. *Bioessays.* 23:526–533.
- Yuan, L., J. Pelttari, E. Brundell, B. Bjorkroth, J. Zhao, J.G. Liu, H. Brismar, B. Daneholt, and C. Hoog. 1998. The synaptonemal complex protein SCP3 can form multistranded, cross-striated fibers in vivo. *J. Cell Biol.* 142:331–339.
- Yuan, L., J.G. Liu, J. Zhao, E. Brundell, B. Daneholt, and C. Hoog. 2000. The murine SCP3 gene is required for synaptonemal complex assembly, chromosome synapsis, and male fertility. *Mol. Cell.* 5:73–83.
- Zickler, D., and N. Kleckner. 1998. The leptotene-zygotene transition of meiosis. *Annu. Rev. Genet.* 32:619–697.